Full paper

Title

Structural analyses of amorphous calcium carbonate before and after removing strontium ions from an aqueous solution

Authors

Yuta SHUSEKI[1], Shinji KOHARA[2]*, Koji OHARA[3], Takahiro OHKUBO[4], Koyo TAKEI[4], Matthew G. TUCKER[5], Alexander I. KOLESNIKOV[5], Marshall T. MCDONNELL[6], Robert L. SACCI[7], Joerg C. NEUEFEIND[5] and Ken TAKEUCHI[1,8]*

[1] Department of Pure and Applied Chemistry, Faculty of Science and Technology, Tokyo University of Science, 2641 Yamazaki, Noda, Chiba 279-8510, Japan
[2] Research Center for Advanced Measurement and Characterization, National Institute for Materials Science (NIMS), 1-2-1 Sengen, Tsukuba, Ibaraki 305-0047, Japan
[3] Diffraction and Scattering Division, Japan Synchrotron Radiation Research Institute (JASRI), Sayo-gun, Hyogo 679-5198, Japan
[4] Graduate School of Engineering, Chiba University, 1-33 Yayoi-cho Inage-ku, Chiba 263-8522, Japan
[5] Neutron Scattering Division, Oak Ridge National Laboratory, Oak Ridge, TN, 37831, USA
[6] Computer Science and Mathematics Division, Oak Ridge National Laboratory, Oak Ridge, TN, 37831, USA
[7] Materials Science and Technology Division, Oak Ridge National Laboratory, Oak Ridge, TN, 37831, USA
[8] Oshamambe Division, Institute of Liberal Arts and Science, Tokyo University of Science, 102-1 Tomino, Oshamambe-cho, Hokkaido 049-3514, Japan

*Corresponding Author.
Ken Takeuchi
E-mail: ken@rs.tus.ac.jp
Shinji Kohara
E-mail: kohara.Shinji@nims.go.jp

Abstract

Amorphous calcium carbonate (ACC) is a precursor of crystalline calcium carbonate; hence, its structural information at the atomic level is very important for controlling the morphology of crystalline calcium carbonate. In this study, we attempted to elucidate the process of Sr extraction from aqueous solution by using ACC for the purpose of removal of radioactive Sr from the contaminated water leaked after the Fukushima Daiichi nuclear accident. The pair distribution functions, $g(r)$ obtained by X-ray and neutron diffraction measurements show that ACC has a structure partially similar to that of monohydrocalcite, suggesting that ACC is transferred to the crystalline calcium carbonate starting from its crystal nucleus. Rietveld analysis of the neutron diffraction data showed that the ACC that removed Sr was crystallized to calcite. However, the Sr-O coordination analyzed using extended X-ray absorption fine structure (EXAFS) implies that the local environment of O around Sr is similar to that in crystalline calcium carbonate aragonite.

Keywords
Calcium carbonate, Adsorbent, Amorphous materials, X-ray diffraction, Neutron diffraction

Body

1. Introduction

Calcium carbonate has various crystal structures: calcite[1] is the most stable phase and aragonite[2] and vaterite[3] are metastable. Monohydrocalcite ($CaCO_3$-1.0H_2O)[4] and ikaite ($CaCO_3$-6.0H_2O)[5] can be found in specific environments such as alkaline salt lakes. In recent years, there have been many research studies on amorphous calcium carbonate (ACC) carried out because amorphous materials have more attractive functions than crystal materials. After the discovery of ACC in 1898[6], many discussions have been done about its physical properties and synthetic methods.[7] The number of studies focusing on the structure of ACC has increased with the development of quantum beam technologies over the past few years.[8-10] Since ACC is a precursor of crystal calcium carbonate, its structural information is essential for controlling the morphology of crystal calcium carbonate. Goodwin et al. discussed the ACC structural model generated by reverse Monte Carlo modeling based on high-energy X-ray diffraction (XRD) and extended X-ray absorption fine structure (EXAFS) data.[11] From the viewpoint that the ACC structure has a significant effect on the crystal growth of calcium carbonate, Tomono et al. evaluated by molecular dynamics simulation the structural changes of ACC induced by additives and water.[12] As mentioned above, the structural analysis of ACC has been widely carried out; however, there are only a few studies on its practical use and fewer on how it captures heavy metal ions.

To remove radioactive Sr from the contaminated water that spilled owing to the Fukushima Daiichi Nuclear Power Plant accident, we have investigated that the Sr^{2+} removal mechanism from an aqueous solution using scallop shell powder, whose main component is $CaCO_3$. A Sr adsorbent prepared using hydroxyapatite[13] or tantalum-doped tungsten oxide[14] has been reported, but these are expensive and, impose a heavy burden on the environment. Thus, such an adsorbent is difficult to be used for the treatment of large amounts of contaminated water. On the other hand, since scallop shell is a natural material and inexpensive, it is a suitable adsorbent for treating considerable amounts of waste water.

We evaluated the Sr^{2+} removability by scallop shell and found that it was greatly improved by amorphizing $CaCO_3$. Moreover, it has been discovered that ACC has a Sr removability about 70 times higher than that of crystalline $CaCO_3$ at an initial Sr^{2+} concentration of 10 mg/L[15].

In this study, we attempted to clarify the process by which ACC removes Sr^{2+} by quantum beam measurements such as synchrotron X-ray/pulsed neutron diffraction in combination with computer simulation.

2. Experimental and simulation procedures

ACC was synthesized by reacting aqueous solution of $CaCl_2$, Na_2CO_3 and NaOH. The concentrations of the solutions were 0.1 mol/dm^3 $CaCl_2$ aq, 0.1 mol/dm^3 Na_2CO_3 aq, and 0.1 mol/dm^3 NaOH aq. To adjust the pH, NaOH aq was added to Na_2CO_3 aq prior to the addition of $CaCl_2$ aq[16]. After the solution became cloudy, the colloidal material was filtered and washed with acetone. The atomic composition of the sample was analyzed by atomic absorption spectrometry (Thermo, iCE3000), thermogravimetric analysis (PerkinElmer, TGA4000), and density measurement (Accupyc II 1340 V2.00). The composition of the sample was $CaCO_3 \cdot 1.0H_2O$ and the density was 2.10 g/cm^3.

To obtain detailed structural information of the amorphous sample, the pair distribution function $g(r)$ (PDF), which provides the probability of finding another atom that exists at a distance r from one atom, was used. To obtain $g(r)$ with high real space resolution, it is necessary to increase the maximum value $Q_{\max}$ of the scattering vector Q (=(4πsinθ)/λ; 2θ; scattering angle; λ; incident wavelength of X-rays or neutrons) as much as possible.[17)] Therefore, in this study, high-energy X-ray diffraction measurement using the BL04B2 beamline (energy: 61.4 keV)[18)] at SPring-8 in Japan and pulsed neutron diffraction (ND) measurement using NOMAD[19)] at Spallation Neutron Source of Oak Ridge National Laboratory in the USA were carried out. The measured data were corrected for absorption, background, and multiple scattering (neutron), and then incoherent scattering was subtracted. Fully corrected data were normalized to obtain the Faber-Ziman[20)] total structure factors $S(Q)$, which can be expressed as

$$S(Q) = \sum_i^n \sum_j^n \frac{c_i c_j b_i b_j}{< b >^2} S_{ij}(Q) = \sum_i^n \sum_j^n W_{ij} S_{ij}(Q) \quad (1)$$

$$< b >^2 = \left(\sum_i^n c_i b_i\right)^2 \quad (2)$$

Here, c_i: the atomic fraction, b_i: the coherent scattering length in ND (atomic form factor in XRD), $S_{ij}(Q)$: partial structure factor.
$g(r)$ was obtained by the Fourier transform of $S(Q)$.

$$g(r) = 1 + \frac{1}{2\pi^2 r\rho} \int_{Qmin}^{Qmax} Q[S(Q) - 1]\sin(Qr)\mathrm{d}Q \quad (3)$$

where ρ_0: the atomic number density.
The reduced pair distribution function $G(r)$, total correlation function $T(r)$, radial distribution function $RDF(r)$, and $g(r)$ have the following relations.

$$G(r) = 4\pi r\rho \cdot (g(r) - 1) \quad (4)$$

$$T(r) = 4\pi r\rho \cdot g(r) \quad (5)$$

$$RDF(r) = 4\pi^2 r\rho \cdot g(r) \quad (6)$$

Since the amount of Sr used in this study is extremely small[13)], we used the EXAFS technique that can measure trace elements with high sensitivity to obtain the inter-atomic distance and coordination number. EXAFS measurements were performed at the Sr K edge using a Si 111 double-crystal monochromator at BL01B1[21)] of SPring-8. Strontium carbonate and strontium oxide were used as references. Data were analyzed using Athena and Artemis[22)].

To generate a structural model of ACC, we performed molecular dynamics (MD) simulation employing the LAMMPS code[23)]. Raiter's[24)] and SPC/Fw[25)] potentials were used for calcium carbonate and water, respectively. The number of particles was 8000 (Ca; 1000, C; 1000, O_C (oxygen atom coordinates to carbon atom); 3000, O_H (oxygen atom coordinates to hydrogen atom): 1000, H; 2000,). The simulation was performed using the NVT-ensemble at 300 K for 10 ns after annealing at 5000 K for 0.1 ps and cooling at 47 K/ps from 5000 K to 300 K. In the structural analysis of crystalline calcium carbonate, $g_{ij}(r)$ was calculated using PDFgui[26)]. The Rietveld analysis of crystalline calcium carbonate after Sr removal was performed using GSAS[27)].

3. Results and discussion

Please insert Fig. 1, 2 here.

Figure. 1 shows the structure factors, $S(Q)$ of ACC obtained by XRD/ ND measurements and MD simulations. For $S^X(Q)$, two sharp peaks can be confirmed at around Q_1=2.22 Å^{-1} and Q_2=3.28 Å^{-1}. Similar peaks are observed at Q=2.39 Å^{-1} and 3.44 Å^{-1} for molten sodium carbonate[28)].The $S(Q)$ obtained by the MD simulation qualitatively agrees with the experimental diffraction data. Fig. 2 shows $G(r)$ obtained from MD simulations and experimental $S(Q)$ obtained by a Fourier transform together with crystalline phase data calculated using PDFgui on the basis of average crystal structures. The relationship between the partial structure factors, $S_{ij}(Q)$ and X-ray and neutron total structure factors, $S^{X,N}(Q)$ are,

$$
\begin{aligned}
S^X(Q)=&0.111S_{\text{Ca-Ca}}(Q)+0.067S_{\text{Ca-C}}(Q)+0.267S_{\text{Ca-Oc}}(Q)+0.022S_{\text{Ca-H}}(Q)\\
&+0.089S_{\text{Ca-Ow}}(Q)+0.010S_{\text{C-C}}(Q)+0.080S_{\text{C-Oc}}(Q)+0.009S_{\text{C-H}}(Q)+0.027S_{\text{C-Ow}}(Q)\\
&+0.160S_{\text{Oc-Oc}}(Q)+0.027S_{\text{Oc-H}}(Q)+0.107S_{\text{Oc-Ow}}(Q)+0.001S_{\text{H-H}}(Q)\\
&+0.009S_{\text{H-Ow}}(Q)+0.018S_{\text{Ow-Ow}}(Q), \qquad (7)\\
S^N(Q)=&0.031S_{\text{Ca-Ca}}(Q)+0.086S_{\text{Ca-C}}(Q)+0.225S_{\text{Ca-Oc}}(Q)-0.097S_{\text{Ca-H}}(Q)+0.075S_{\text{Ca-Ow}}(Q)\\
&+0.060S_{\text{C-C}}(Q)+0.314S_{\text{C-Oc}}(Q)-0.135S_{\text{C-H}}(Q)+0.105S_{\text{C-Ow}}(Q)+0.411S_{\text{Oc-Oc}}(Q)\\
&-0.353S_{\text{Oc-H}}(Q)+0.274S_{\text{Oc-Ow}}(Q)+0.076S_{\text{H-H}}(Q)-0.118S_{\text{H-Ow}}(Q)+0.274S_{\text{Ow-Ow}}(Q). \qquad (8)
\end{aligned}
$$

Please insert Fig. 3 here.

The assumption weighting factors, W_{ij} were calculated using an atomic number in the case of XRD because the atomic form factor $f(Q)$ has Q-dependent. X-rays are sensitive to Ca, which has a large atomic number, but not to light elements such as hydrogen. On the other hand, since neutrons are sensitive to oxygen and hydrogen, the peak of C-O_c in Fig. 2 is sharp, and the O_w-H correlation peak is clearly visible for $G^N(r)$. Peak 1 $G^N(r)$ is negative because the H-O_H weighting factor is negative (see eq. 8). The peaks observed for the experimentally obtained $G^{X,N}(r)$ can be assigned on the basis of $G^{X,N}(r)$ of crystalline calcium carbonate: [peak 1] H-O_w at 0.95 Å, [peak 2] C-O_c at 1.26 Å, [peak 3] H-H at 1.63 Å, [peak 4] Oc-Oc at 2.22 Å, [peak 5] Ca-Oc or O_w 2.24 Å, and [peak 6] Ca-C, O_c-O_w, and O_w-O_w at 2.92 Å. Fig. 3 shows the structural model of ACC generated by MD simulation. As can be seen in the figure, CO_3^{2-} ions form a network via Ca ions. Moreover, it is found that the Ca-O coordination shows a variation, which is inherent in disordered materials.

Please insert Fig. 4,5 here.
Please insert Table 1 here.

The distributions of the Ca-O coordination number $N_{\text{Ca-O}}$ calculated on the basis of structure of ACC obtained by MD simulation are shown in Fig. 4. It is found that Ca atoms are coordinated by about 5-7 O_c and 0-3 O_w. Table 1 shows the Ca-O atomic distance of crystalline calcium carbonate, the average coordination number $N_{\text{Ca-O}}$, crystal system, and density. The average Ca-O coordination numbers for the ACC are $N_{Ca\text{-}Oc}$=5.6 and $N_{Ca\text{-}Ow}$=1.2; these are smaller than those in the crystalline monohydrocalcite, which is a characteristic typical of disordered materials. The average $N_{Ca\text{-}O}$ (Oc and Ow) in the MD model is slightly larger than that in the RMC model reported by Goodwin et al[11)]. Moreover, the distribution of $N_{Ca\text{-}O}$ in the RMC model is broader than that in our MD model, because RMC generates the most disordered structure[29)], which is consistent with a given data set of diffraction and geometrical constraints.

Fig. 5(A) shows the partial pair distribution functions of Ca-O, $g_{Ca\text{-}O}(r)$ of ACC, and crystalline calcium carbonate together with atomic coordinates, which represent typical atomic distances between Ca and O atoms in crystal structures (Fig. 5(B) and 5(C)). The first peak of $g_{Ca\text{-}O}(r)$ is observed at 2.36 Å, which is close to those of calcite and monohydrocalcite. However, the second peak of ACC is broad, and a similar trend is observed only in monohydrocalcite. Moreover, calcite shows that one O of CO_3^{2-} is coordinated to Ca (Fig. 5(B)), whereas one or two O are coordinated to Ca in monohydrocalcite (Fig. 5(C)). Owing to the difference in coordination number, the second peak of monohydroclaicite is broad and the O atoms in the second coordination shows a wide distribution of 3.6-4.5 Å. Therefore, from the O coordination number, the MD model for ACC has a structure close to those of calcite and monohydrocalcite in the first coordination, but in the second coordination the model has a structure similar to that of monohydrocalcite.

Please insert Fig. 6 here.
Please insert Table 2 here.

The structure of ACC after removing Sr was evaluated using ND. Fig. 6 shows the results of the Rietveld analysis of ACC samples stirred in deionized (DI) water (A) and Sr solution (B). Note that the atomic composition of the sample stirred in Sr solution analyzed by atomic absorption spectroscopy is $Ca_{0.99}Sr_{0.01}CO_3$. As can be seen in Figs. 6 (A) and (B), sharp Bragg peaks are observed for both samples, suggesting that ACC dried after the stirring was crystallized in the aqueous solution regardless of the presence of Sr in solution. It is demonstrated from these results that ACC transformed into anhydrous crystalline calcium carbonate. Table 2 shows the space groups and lattice constants obtained from Rietveld analysis results. It is found that both samples show the same space group *R3c*, and the lattice constants remain almost the same even after the addition of Sr, because the amount of Sr contained in calcium carbonate is very small. Hashimoto et al.[30)] have reported that ACC becomes a calcite structure directly or via vaterite when synthesized at a water temperature of 30 ℃ or below. The ACC in this study has a structure similar to that of monohydrocalcite, implying that structural transition occurred from its crystal nucleus. Therefore, it is presumed that the ACC in the Sr solution was directly transferred to the calcite structure. Johannes et al.[31)] reported that hydrous ACC first loses water molecules when it crystallizes in air, and it is transferred into a calcite structure via anhydrous ACC. Since the hydrous ACC was transferred to anhydrous crystalline calcium carbonate after stirring in an aqueous solution in our study, we propose that ACC follows the process of hydrous ACC → anhydrous ACC → calcite.

Please insert Fig. 7 here.

Since it is not possible to clarify the coordination state of Sr in calcium carbonate by Rietveld analysis, we evaluated it by EXAFS, which can detect trace elements with high sensitivity. Fig. 7 shows the EXAFS data, Sr K edge EXAFS function $k^3\chi(k)$ and fourier transform magnitude $\chi(R)$.

The Sr-O inter-atomic distance is $r_{Sr\text{-}O}$=2.52±0.006 Å and the Sr-O coordination number is $N_{Sr\text{-}O}$=9.42±0.7, suggesting that the local environment of O around Sr in calcium carbonate has a structure similar to that of the O coordinate of aragonite in crystalline calcium carbonate (see Table 1). This behavior implies that the local environment of O around Sr is different from the model proposed by Hashimoto et al.[27] It is unlikely that the calcite, which is the most stable phase of crystalline calcium carbonate, transfers to Aragonite. Therefore, it is indicated that at the local environment of O around Sr, the crystallization process is hydrous ACC → anhydrous ACC → aragonite. Moreover, Sr is considered suppress the crystal transition from the metastable aragonite to the stable calcite.

4. Conclusion

In this study, we attempted to analyze the structure of amorphous calcium carbonate before and after removing Sr by MD simulation, Rietveld analysis, and EXAFS measurements based on the experimental XRD and ND data for ACC. The MD model shows that ACC has a structure partially similar to that of monohydrocalcite, and its crystal nucleus might be the starting point of crystal transition. In addition, ACC loses water molecules and crystallizes when placed in an aqueous solution, suggesting the following crystallization process: hydrous ACC → anhydrous ACC → calcite. On the other hand, it is clarified that the local environment of O around Sr is similar to the oxygen coordination of aragonite, suggesting that the process of crystallizing ACC is strongly affected by the presence or absence of Sr. To clarify the crystallization process associated with Sr removal, it is necessary to analyze the reaction pathway using the free-energy calculation analysis method[32] based on the three-dimensional atomistic structure before and after Sr removal generated in this study. We are confident that this study, which combines experiments and the computational approach plays an important role in deriving the basis for the analysis of disordered and ordered phases in ACC associated with cation element removal.

Acknowledgments

The synchrotron radiation experiments were performed at BL01B1 and BL04B2 of SPring-8 with the approval of the Japan Synchrotron Radiation Reserch Institute (JASRI) (Proposal Nos. 2018B2095, 2019B1562 and 2019B2091). The pulsed neutron scattering measreuments were conducted at NOMAD (Proposal Nos. IPTS-22206 and 22235), Sapallation Neutron Source, a DOE Office of Science User Facilities operated by the Oak Ridge National Laboratory. This research was supported by Hosokawa Powder Technology Foundation (Grant number 19505) and Showa Ikeda Memorial Foundation (to Y.S.). This study was partially supported by a Grant-in-Aid for Transformative Research Areas (A) “Hyper-Ordered Structures Science” (Grant No. 20H05881 and 20H05878). The supports of Dr. T. Ina, H. Masai, and Dr. M. M. Everett in experiments are gratefully appreciated. R. L. S. was supported by the Department of Energy, Office of Science, Basic Energy Sciences, Materials Sciences and Engineering Division.

References

1) S. A. Markgraf and R. J. Reeder, *Am. Mineral.*, **70**, 590–600 (1985).
2) B. Pokroy, J. S. Fieramosca, R. B. Von Dreele, A. N. Fitch, E. N. Caspi and E. Zolotoyabko, *Chem. Mater.*, **19**, 3244–3251 (2007).
3) H. J. Meyer, *Angew. Chem.*, **71**, 678–679 (1959).

4) I. P. Swainson, *Am. Mineral*., **93**, 1014–1018 (2008).
5) N. Tateno and A. Kyono, *J. Mineral. Petrol. Sci*., **4**, 157–168 (2014).
6) H. E. Sturcke, Process of preparing amorphous carbonate of lime from residues, U. S. Patent 603. 226., 1898-04-26.
7) T. Yasue, A. Mamiya, Y. Takehashi and R. Tsukisaka, Y. Arai, *Chem. Soc. Jpn*., **7**, 1107–1113 (1984).
8) H. W. Wang, L. L. Daemen, M. C. Cheshire, M. K. Kidder, A. G. Stack, L. F. Allard, J. Neuefeind, D. Olds, J. Liu and K. Page, *Chem. Commun*., **53**, 2942–2945 (2017).
9) A. C. S. Jensen, S. Lmberti, S. F. Parker, E. Schneck, Y. Politi, P. Fratzl, L. Bertinetti and W. J. E. M. Habraken, *J. Phys. Chem. C*, **122**, 3591–3598 (2018).
10) J. W. Singer, A. O, Yazaydin, R. J. Kirkpatrick and G. M. Bowers, *Chem. Mater*., **24**, 1828–1836 (2012).
11) A. L. Goodwin, F. M. Michel, B. L. Phillips, D. A. Keen, M. T. Dove and R. J. Reeder, *Chem. Mater*., **22**, 3197–3205 (2010).
12) H. Tomono, H. Noda, F. Zhu, T. Sakamoto, T. Nishimura and T. Kato, *J. Phys. Chem. B*, **117**, 14849–14856 (2013).
13) T. Ono, *Isotope News*, **743**, 19-20 (2016).
14) X. Li, W. Mu, X. Xie, B. Liu, H. Tang, G. Zhou, H. Wei, Y. Jian and S. Luo, *J Hazard. Mater*., **264**, 245-252 (2014).
15) Y. Shuseki, F. Mihara, A. Yasumori, Y. Idemoto, S. Koura and K. Takeuchi, *J. Ceram. Soc. Jpn*., **128**, 560–564 (2020).
16) Y. Kojima, A. Kawanobe, T. Yasue and Y. Arai, *J. Ceram. Soc. Jpn.*, **101**, 1145–1152 (1993).
17) D. A. Keen, *J. Appl. Cryst*., **34**, 172–177 (2001).
18) K. Ohara, Y. Onodera, M. Murakami and S. Kohara, *J. Phys.: Condens. Matter*, **33**, 383001 (2021).
19) J. Neuefeind, M. Feygenson, J. Carruth, R. Hoffmann and K. K. Chipley, *Nucl. Instrum. Meth. B*, **287**, 68–75 (2012).
20) T. E. Faber and J. M. Ziman, *Philos. Mag*., **11**, 153–173 (1965).
21) T. Uruga, H. Tanida, Y. Yoneda, K. Takeshita, S. Emura, M. Takahashi, M. Harada, Y. Kubozono, T. Tanako, T. Yamamoto, H. Maeda, O. Kamishima, Y. Takabayashi, Y. Nakata, H. Kimura, S. Goto and T. Ishikawa, *J. Synchrotron Radiat.*, **6**, 143–145 (1999).
22) B. Ravel and M. Newville, *J. Synchrotron Radiat*., **12**, 537–541 (2005).
23) S. Plimpton, *J. Comput. Phys.*, **117**, 1–19 (1995).
24) P. Raiteri, R. Demichelis and J. D. Gale, *J. Phys. Chem. C*, **119**, 24447–24458 (2015).
25) Y. Wu, H. L. Tepper and G. A. Voth, *J. Chem. Phys.*, **124**, 024503 (2006).
26) C. L. Farrow, P. Juhas, J. W. Liu, D. Bryndin, E. S. Božin, J. Bloch, T. Proffen, S. J. L. Billinge, *J. Phys.: Condens. Matter*, **19**, 335219 (2007).
27) B. H. Toby, *J. Appl. Cryst*., **34**, 210–213 (2001).
28) M. C. Wilding, M. Wilson, O. L. G. Alderman, C. Benmore, J. K. R. Weber, J. B. Parise, A. Tamalonis and L. Skinner, *Sci. Rep*,. **6**, 24415 (2016).
29) M. T. Dove, M. G. Tucker and D. A. Keen, Eur. J. Mineral., 14, 331-348 (2002).
30) R. Hashimoto, M. Morita, O. Umezawa and S. Motoda, *J. Jpn. Inst. Metal. Mater.*, **2**, 89–96 (2017).
31) J. Ihli, W. C. Wong, E. H. Noel, Y. Y. Kim, A. N. Kulak, H. K. Christenson, M. J. Duer and F. C. Meldrum, *Nat. Commun*., **5**, 3169 (2014).
32) A. Laio and F. L. Gervasio, *Rep. Prog. Phys*., **71**, 126601 (2008).

Caption list

Fig. 1 X-ray and Neutron total structure factors, $S^{X,N}(Q)$ for amorphous $CaCO_3$.

Fig. 2 Reduced pair distribution functions, $G^{X,N}(r)$ for amorphous $CaCO_3$ obtained by diffraction experiments (cyan) and MD simulations (magenta) together with those for monohydrocalcite (MHC, crystal)[4)], vaterite (crystal)[3)], aragonite (crystal)[2)], and calcite (crystal)[1)] on the basis of crystal structures calculated using PDFgui[22)].

Fig. 3 MD-generated atomic structure for amorphous $CaCO_3$. (A) large scale, (B) small scale.

Fig. 4 Distribution of coordination numbers of O_c and O_w around a Ca for amorphous $CaCO_3$, calculated from MD simulation.

Fig. 5 (A) Partial pair distribution functions for Ca-O, $g_{Ca\text{-}O}(r)$ obtained by MD simulation, together with those for monohydrocalcite, vaterite, aragonite, and calcite determined on the basis of crystal structures using PDFgui, and (B, C) Ca coordination environment of calcite and monohydrocalcite.

Fig. 6 Rietveld refinement patterns of $CaCO_3$ (stirred in Diwater:A) and $Ca_{0.99}Sr_{0.01}CO_3$ (stirred in Sr solution:B).

Fig. 7 The EXAFS $k^3\chi(k)$:(A) and $\chi(r)$:(B) measured at Sr K edge together with the results of parameter fitting for $Ca_{0.989}Sr_{0.011}CO_3$.

Table 1 The $r_{Ca\text{-}O}$, $N_{Ca\text{-}O}$, crystal system, and density of crystalline and amorphous calcium carbonate.

Table 2 Refined structure parameters of $CaCO_3$ (stirred in Diwater) and $Ca_{0.99}Sr_{0.01}CO_3$ (stirred in Sr solution).

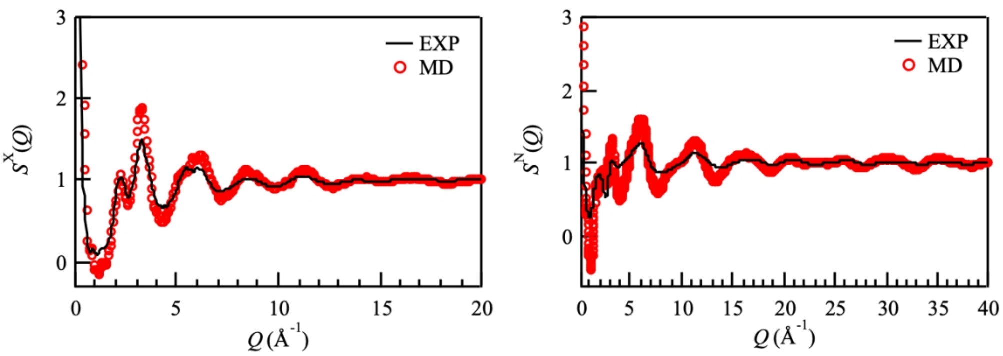

Fig. 1 X-ray and Neutron total structure factors, $S^{X,N}(Q)$ for amorphous $CaCO_3$.

374x130mm (130 x 130 DPI)

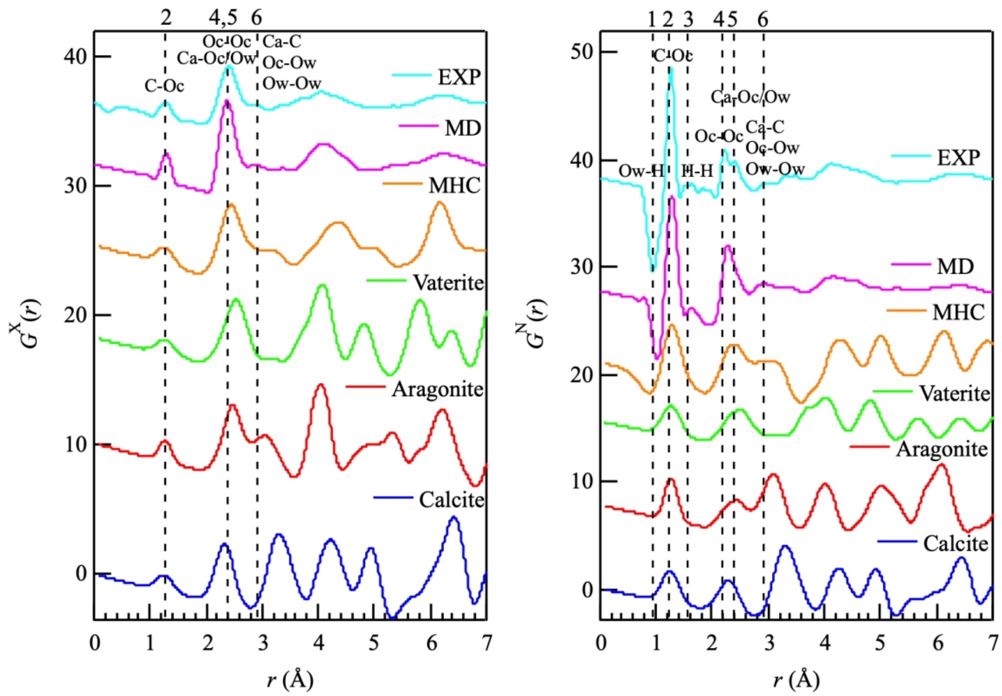

Fig. 2 Reduced pair distribution functions, $G^{X,N}(r)$ for amorphous $CaCO_3$ obtained by diffraction experiments (cyan) and MD simulations (magenta) together with those for monohydrocalcite (MHC, crystal)[4)], vaterite (crystal)[3)], aragonite (crystal)[2)], and calcite (crystal)[1)] on the basis of crystal structures calculated using PDFgui[22)].

387x267mm (130 x 130 DPI)

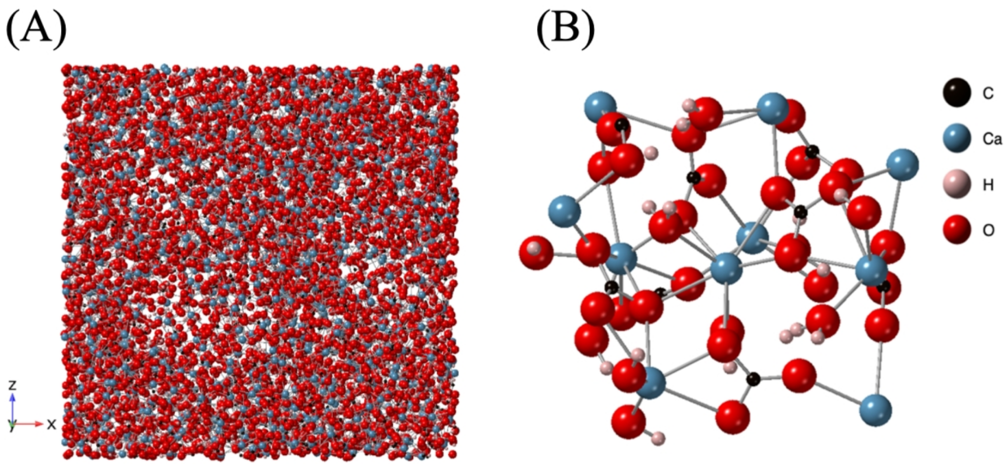

Fig. 3 MD-generated atomic structure for amorphous $CaCO_3$. (A) large scale, (B) small scale.

357x164mm (130 x 130 DPI)

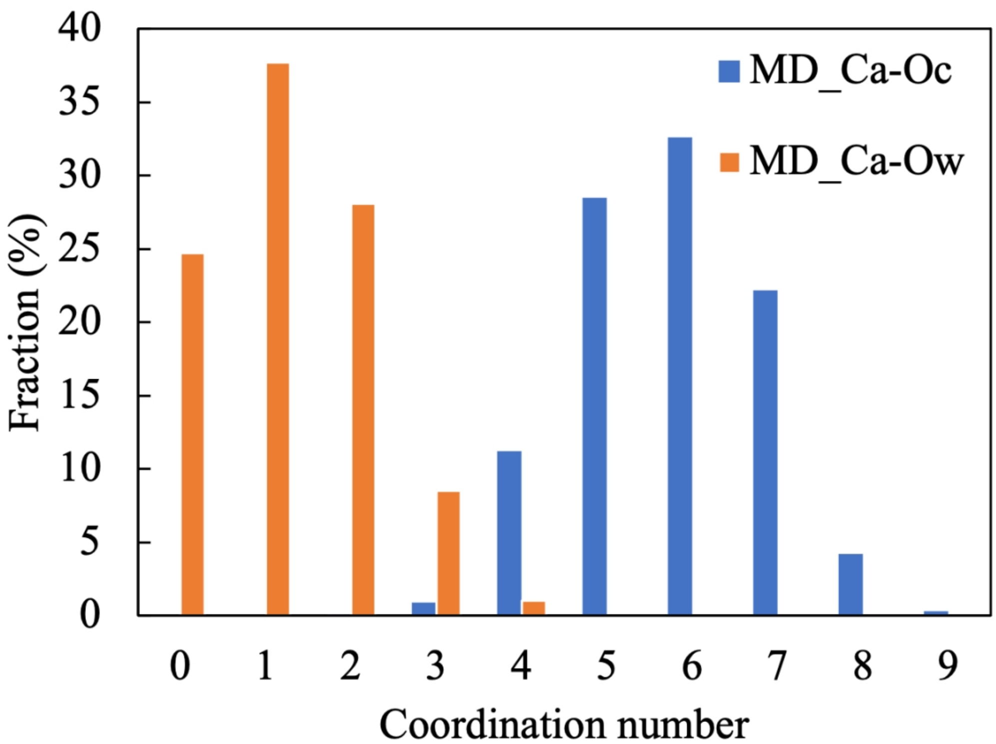

Fig. 4 Distribution of coordination numbers of O_C and O_W around a Ca for amorphous $CaCO_3$, calculated from MD simulation.

248x184mm (130 x 130 DPI)

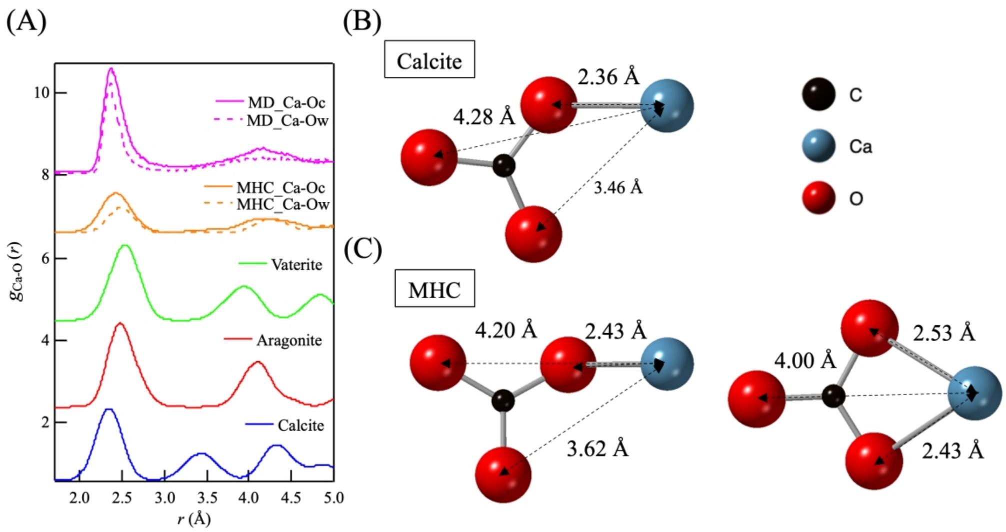

Fig. 5 (A) Partial pair distribution functions for Ca-O, $g_{Ca\text{-}O}(r)$ obtained by MD simulation, together with those for monohydrocalcite, vaterite, aragonite, and calcite determined on the basis of crystal structures using PDFgui, and (B, C) Ca coordination environment of calcite and monohydrocalcite.

545x286mm (130 x 130 DPI)

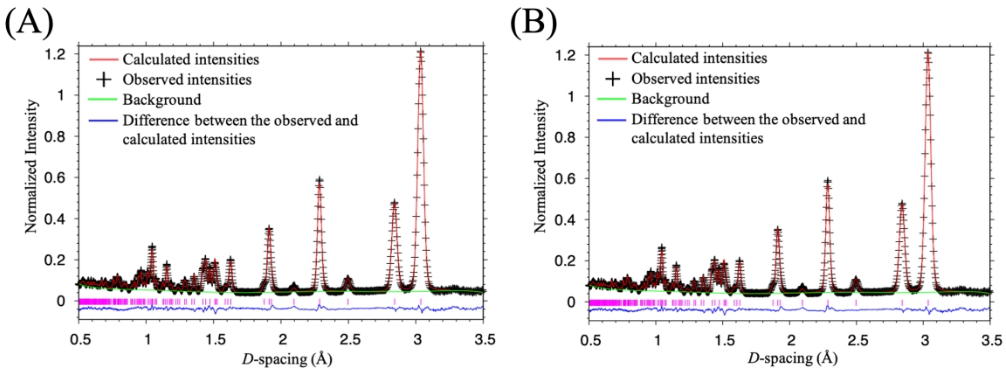

Fig. 6 Rietveld refinement patterns of $CaCO_3$ (stirred in DI-water:A) and $Ca_{0.99}Sr_{0.01}CO_3$ (stirred in Sr solution:B).

448x163mm (130 x 130 DPI)

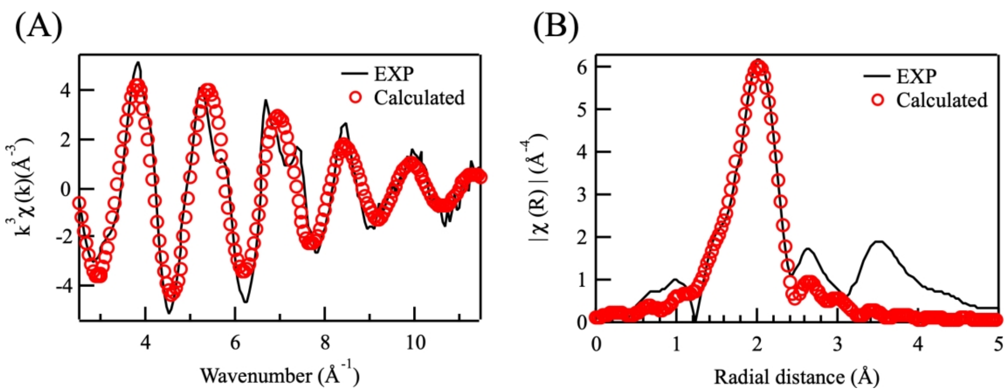

Fig. 7 The EXAFS $k^3\chi(k)$:(A) and $\chi(R)$:(B) measured at Sr K edge together with the results of parameter fitting for $Ca_{0.989}Sr_{0.011}CO_3$.

462x175mm (130 x 130 DPI)

Table 1 The $r_{\text{Ca-O}}$, $N_{\text{Ca-O}}$, crystal system, and density of crystal and amorphous calcium carbonate.

	Calcite ($CaCO_3$)	Aragonite ($CaCO_3$)	Vaterite ($CaCO_3$)	Monohydro calcite ($CaCO_3 \cdot 1.0H_2O$)	Amorphous $CaCO_3$ ($CaCO_3 \cdot 1.0H_2O$)
$r_{\text{Ca-Oc/Ow}}$ (Å)	2.34	2.47	2.53	2.42 (Ca-Oc) 2.48 (Ca-Ow)	2.36 (Ca-Oc) 2.36 (Ca-Ow)
Coordination number N	6	9	8	8 $N_{\text{Ca-Oc}}$=6 $N_{\text{Ca-Ow}}$=2	6.8 $N_{\text{Ca-Oc}}$=5.6 $N_{\text{Ca-Ow}}$=1.2
Crystal system	Trigonal	Orthorhombic	Orthorhombic	Trigonal	-
Density (g/cm^3)	2.71	2.92	2.65	2.42	2.10

Table 2 Refined structure parameters of $CaCO_3$ (stirred in DI-water), $Ca_{0.99}Sr_{0.01}CO_3$ (stirred in Sr solution).

Sample (Composition)	Space group	*a*=*b* (Å)	*c* (Å)	R_{wp} (%)	R_e (%)
In DI-water ($CaCO_3$)	*R3c*	4.99573(14)	17.05871(59)	4.55	3.50
In Sr solution ($Ca_{0.99}Sr_{0.01}CO_3$)	*R3c*	4.99573(14)	17.05871(59)	4.55	3.52